

UNIVERSITY OF VICTORIA

ELEC 340

APPLIED ELECTROMAGNETICS AND PHOTONICS

Lab 2 - Uniform Plane Waves

Instructor:

Dr. Poman So

A.K. BLANKEN V00809798

T. STEPHEN V00812021

A01 - B03

February 24, 2016



University
of Victoria

1 Objective

This experiment will use a MEFiSTo simulation to investigate the propagation of an electromagnetic wave through a waveguide. The results of the simulation will validate the Helmholtz equation and provide insight into the propagation properties of plane waves.

2 Introduction

Faraday's and Ampere's Laws can be applied [1, pp. 15-16] to a medium with constant permittivity and permeability to yield the Helmholtz equation:

$$\nabla^2 \tilde{\mathbf{E}} = -\omega^2 \mu \epsilon \tilde{\mathbf{E}} = \gamma^2 \tilde{\mathbf{E}}. \quad (1)$$

This relation implies that the electric field and the magnetic field described by Faraday's and Ampere's Law form an electromagnetic wave that varies in time. The amplitude of the waves relate by the intrinsic impedance of the material. The intrinsic impedance is a material property that is calculated using the permittivity and permeability of the material.

The amplitude of the waves, as well as their phase difference, describe their polarization. In the most general case, each wave has a different amplitude and the phase shift is any angle between 0 and π radians. This corresponds to elliptical polarization. Specific amplitudes and phase angles correspond to special types of polarization: a phase angle of 0 or π corresponds to linear polarization and a phase angle of $\pm \frac{\pi}{2}$ with equal amplitudes corresponds to circular polarization.

3 Procedure

3.1 Uniform plane waves in a parallel plate structure

A perfect parallel plate wave guide is created in MEFiSTo by bounding a region of air with opposite, perfect electrical and magnetic boundaries. The ends of the waveguide are covered with an absorbing boundary. A wave source fills a vertical slice of the waveguide and will act on the transverse and parallel animation regions. This arrangement is shown in Fig. 1, with

the bottom electrical boundary, animation regions and source present.

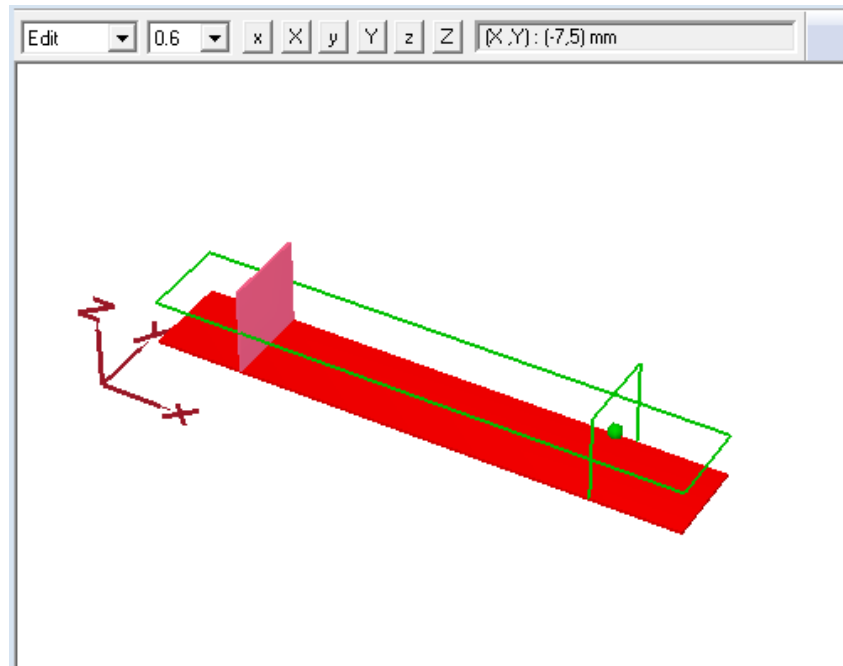


Figure 1: Perfect waveguide with dimensions 60 mm \times 10 mm \times 10 mm

The source emits a wave with $f = 15$ GHz that travels through the medium, bounded by the walls of the waveguide. The solid red color of the yz -animation plane in Fig. 2 shows that the wave travels as a plane wave from its origin through the waveguide.

The wave that is emitted from the source looks like a plane wave when we look at the small portion of it that is displayed in the y - z animation region. The solid red colour indicates an infinite plane wave. This agrees with the theory that a spherical wave can be approximated as a plane wave in the far field region as well as when looking at only a small portion of the wave.

The physical properties of the propagation medium can be determined by examining the wave structure from Fig. 2

With this color scheme, blue regions indicate minima and maxima of the wave. There are 20 grid square between adjacent blue regions in Fig. 3, corresponding the distance between a peak and trough. At 0.5 mm mesh resolution, this indicates that $\lambda = 20$ mm.

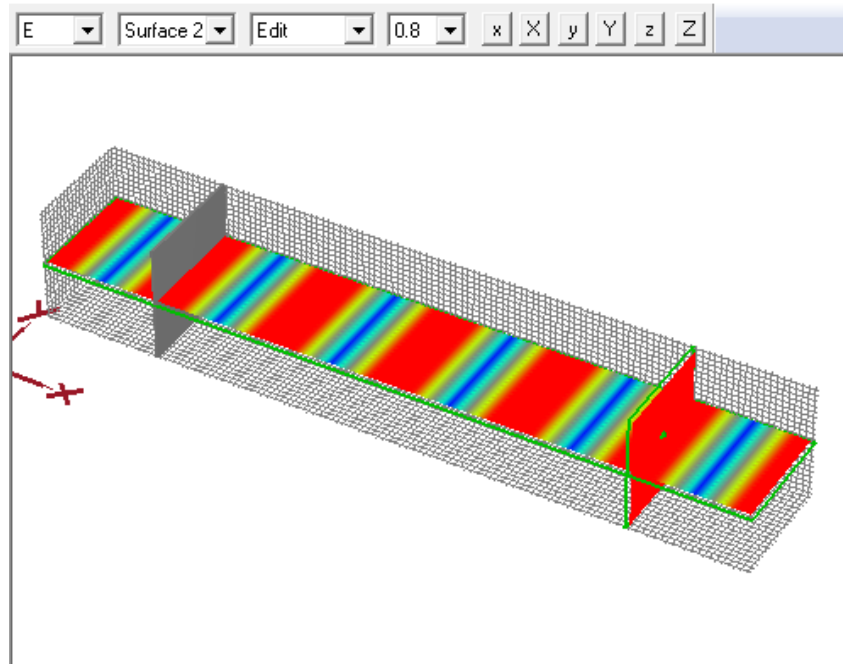


Figure 2: Wave propagation in air-filled waveguide

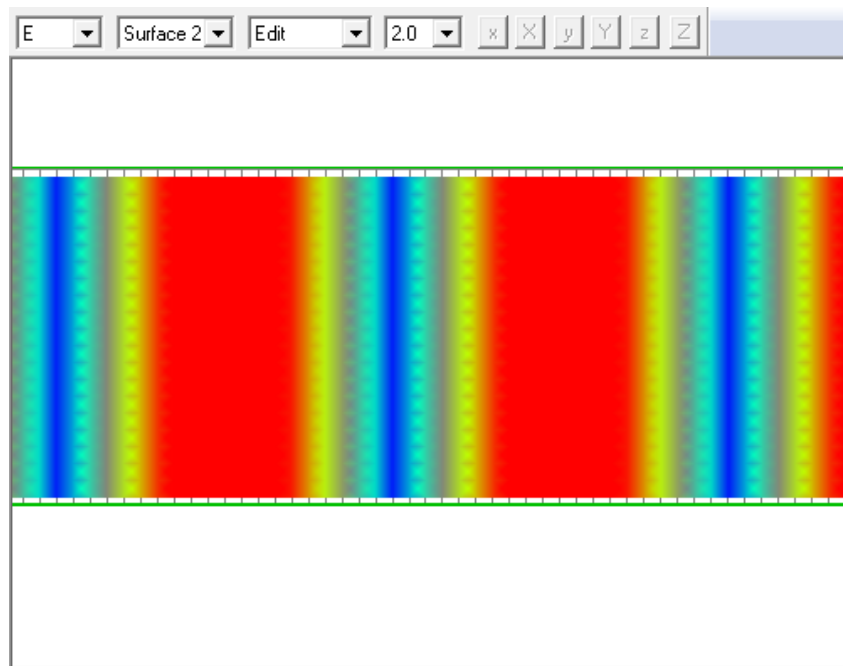


Figure 3: xy view of propagation in Fig. 2, with 0.5 mm mesh

3.2 Waves in a non-ideal parallel plate structure

Removing the magnetic sidewalls from the waveguide allows the wave energy to escape the confines of the guide. When this change is made the wave propagation appears spherical near the source. As the energy moves away from the source, the propagation becomes more planar. This can be seen in Fig. 4(a). Fig. 4(b) shows that the orientation of all \vec{E}_z are identical but their magnitude is not.

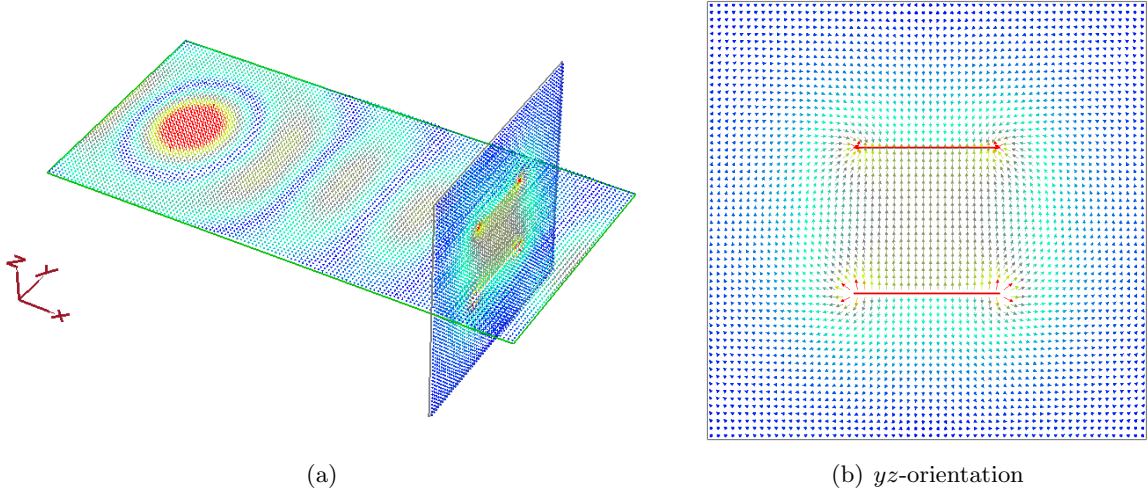


Figure 4: Propagation in a non-ideal parallel plate

3.3 Dielectric and lossy media

The narrow-wide arrangement from Section 3.2 is changed to include a lossy dielectric between the top and bottom electric boundaries. The boundaries with dielectric are shown in Fig. 5.

Propagation in the dielectric is shown in Fig. 6.

The wave attenuates as it travels through the waveguide as a result of $\sigma > 0$.

4 Discussion

Task 4 Compare the phase velocity to what you found in Section 3.1.

By recording the distance traveled by a wave peak in one step of the animation, we found that:

$$u_{ph} = \frac{\Delta x}{\Delta t} = \frac{0.5 \text{ mm}}{0.166 \text{ ps}} = 3.01 \times 10^8 \text{ m s}^{-1}.$$

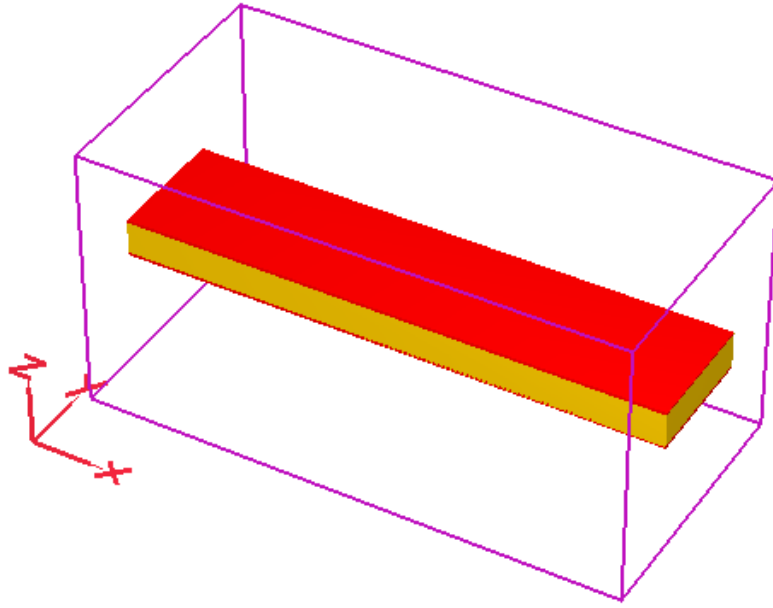


Figure 5: Waveguide containing a lossy dielectric material

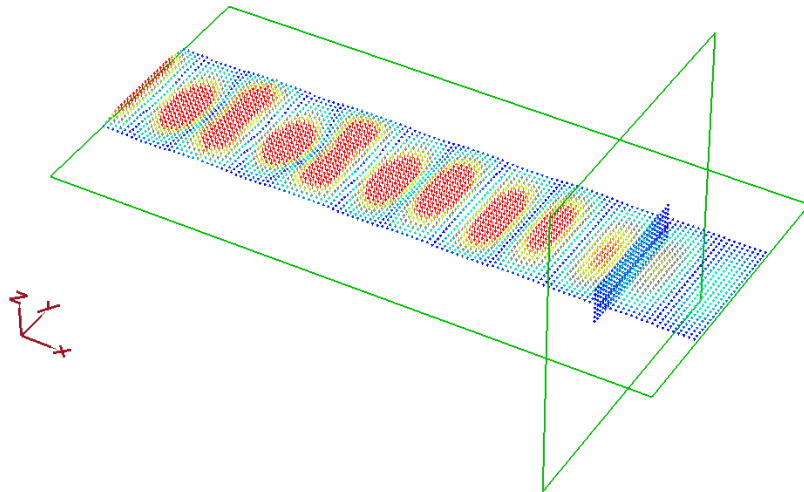


Figure 6: Propagation in a waveguide filled with a dielectric where $\epsilon_r = 4$ and $\sigma = 0.5$

We found that $\lambda = 20$ mm in Section 3.1 which implies that $u_{ph} = c_0$. The discrepancy between the two numbers is likely the result of a rounding error in MEFiSTo.

Task 7 *Reduce the plate spacing to 4 mm and increase the width to 14 mm in the environment used for Section 3.2. Does the far field in the xy and yz planes behave like a uniform plane wave?*

Narrowing the gap between the electric field boundaries and widening them creates the propagation patterns shown in Fig. 7.

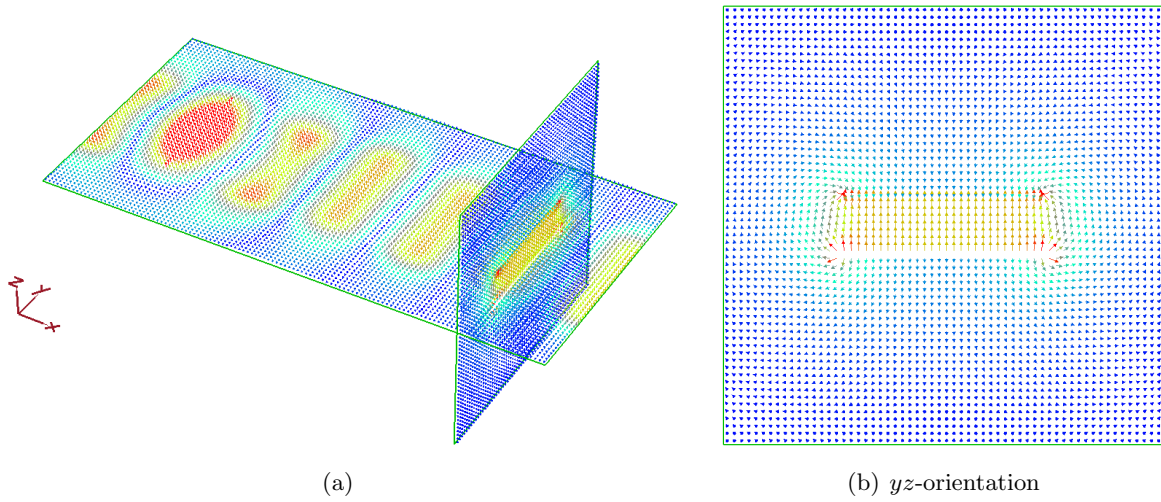


Figure 7: Propagation in a non-ideal, narrow parallel plate

The magnitude of the waves in Fig. 7(a) is greater than those in Fig. 4(a) and the groups have a much shorter and wider region of similar magnitude. Fig. 7(b) confirms that both the direction and magnitude of the wave are similar far from the source. Changing the electric field arrangement to make the separation smaller and boundaries wider has restored the plane wave behavior for the region between the boundaries.

Task 8 *Determine α and β for the waveguide with dielectric from Section 3.3.*

The lab manual suggests using Fig. 8 to determine the attenuation of the wave with equations (2) and (3).

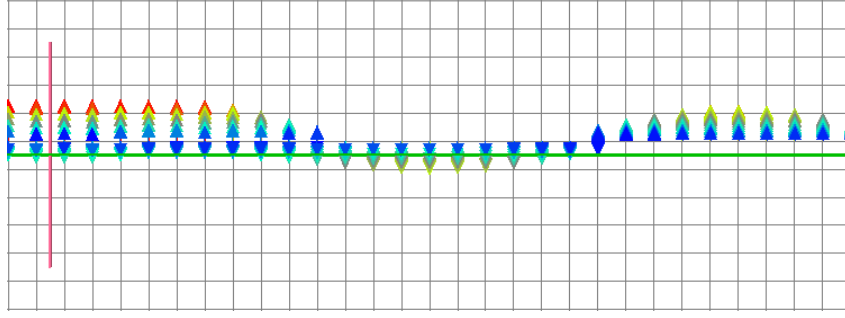


Figure 8: xz view of Fig. 6

$$\alpha = \frac{\ln \left(\frac{E_z(x_1)}{E_z(x_2)} \right)}{m\Delta x} \quad (2)$$

$$\beta = \frac{2\pi}{\lambda} \quad (3)$$

This method poses a problem since the magnitude of the electric field is not displayed on the graph. Determining the ratio of two points is extremely imprecise.

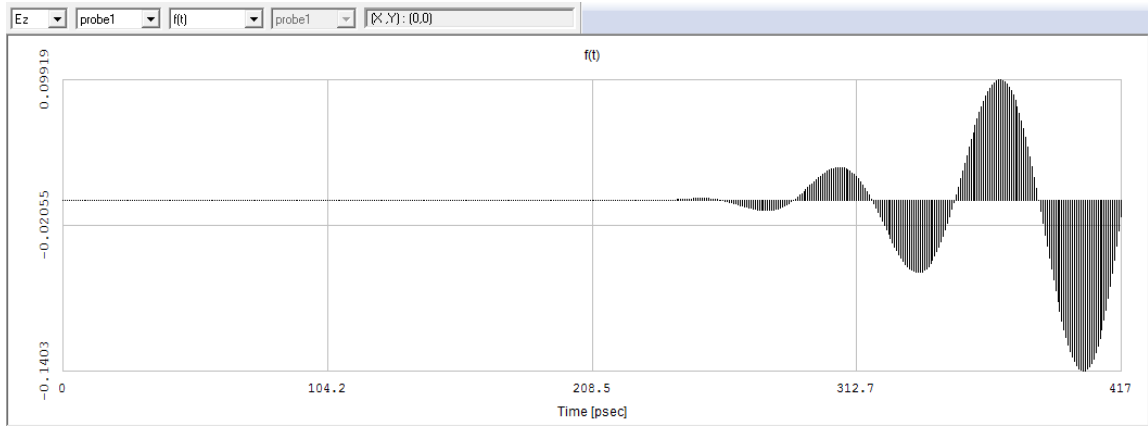
In order to obtain more accurate measurements of E_z , a second probe was added to the animation 5 mm closer to the source than the probe in Fig. 1. The E_z response at both probes is shown in Fig. 9.

Using the peak positive value for both probes with (2) gives:

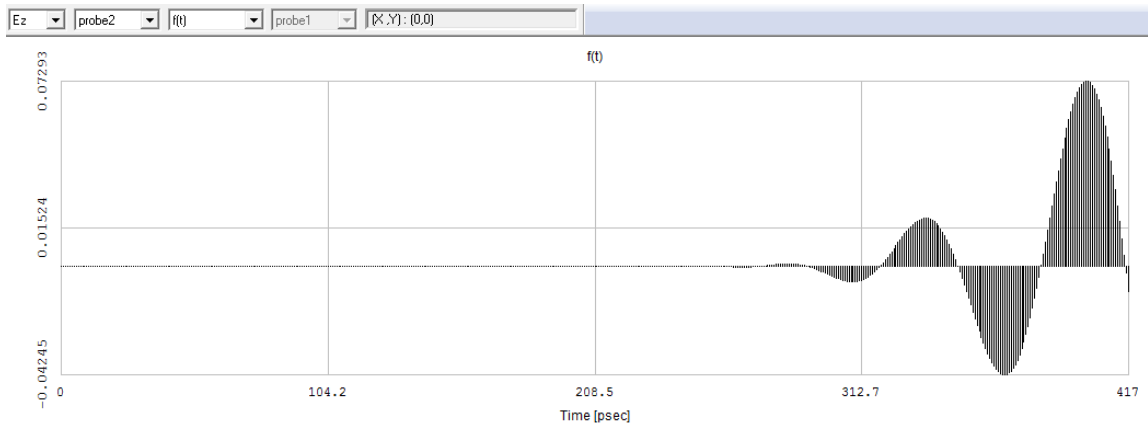
$$\alpha = \frac{\ln \left(\frac{0.09919 \text{ V m}^{-1}}{0.07293 \text{ V m}^{-1}} \right)}{5 \text{ mm}} = 55.9 \text{ Np m}^{-1}.$$

Using the same method for determining wavelength as in Section 3.1, $\lambda = 10 \text{ mm}$. Substitution in (3) yields:

$$\beta = \frac{2\pi}{\lambda} = 628.31 \text{ rad m}^{-1}.$$



(a) 35 mm



(b) 40 mm

Figure 9: E_z response at different distances from source

Task 9 Compare the results of Task 8 to the theoretical values.

The attenuation and phase constants are:

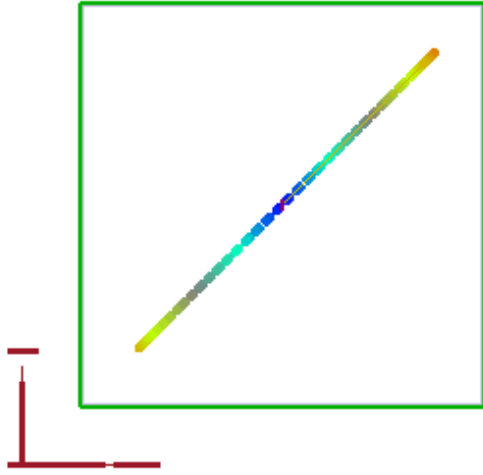
$$\begin{aligned}
 \alpha &= \frac{\omega\sqrt{\mu\epsilon}}{\sqrt{2}} \sqrt{\sqrt{1 + \left(\frac{\sigma}{\omega\epsilon}\right)^2} - 1} \\
 &= \frac{\omega\sqrt{\epsilon_r}}{c_0\sqrt{2}} \sqrt{\sqrt{1 + \left(\frac{\sigma}{\omega\epsilon_0\epsilon_r}\right)^2} - 1} \\
 &= \frac{2\pi \cdot 15 \text{ GHz} \cdot \sqrt{4}}{c_0\sqrt{2}} \sqrt{\sqrt{1 + \left(\frac{0.5}{2\pi \cdot 15 \text{ GHz} \cdot \epsilon_0 \cdot 4}\right)^2} - 1} \\
 &= 46.96 \text{ Np m}^{-1}
 \end{aligned}$$

$$\begin{aligned}
 \beta &= \frac{\omega\sqrt{\mu\epsilon}}{\sqrt{2}} \sqrt{\sqrt{1 + \left(\frac{\sigma}{\omega\epsilon}\right)^2} + 1} \\
 &= 630.50 \text{ rad m}^{-1}
 \end{aligned}$$

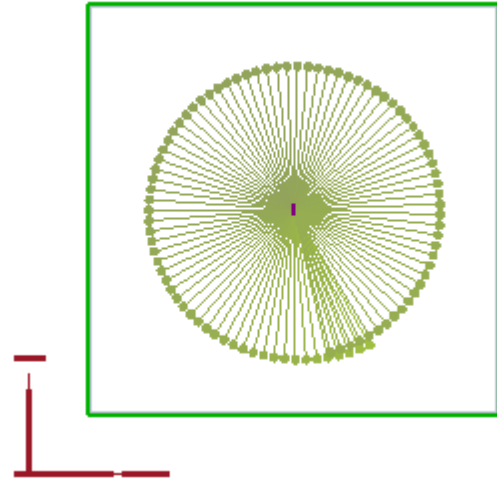
These values agree with the results from Task 8. The error is likely the result of the grid-space-count method of determining λ .

Task 10 Modify the waves in *Polarization_TE.mef* to produce various kinds of polarizations

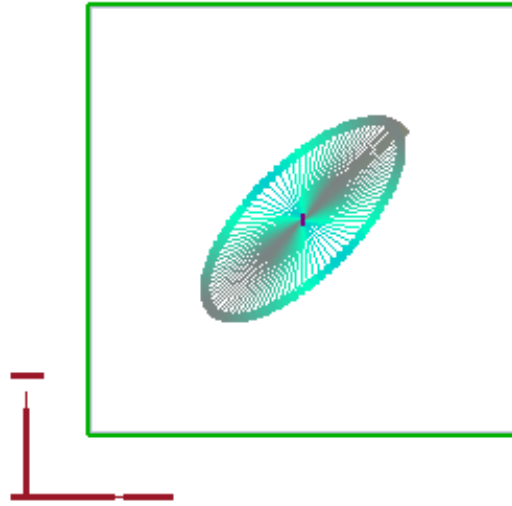
Fig. 10 shows the result of changing E_x and E_y .



(a) $A = 1, \phi_{\Delta} = 0^{\circ}$



(b) $A = 1, \phi_{\Delta} = -90^{\circ}$



(c) $A = 1, \phi_{\Delta} = 45^{\circ}$

Figure 10: Various polarizations of a propagating electric field

5 Conclusion

The simulation was an effective tool to see how waves propagate in free space vs. in a dielectric. The results of a wave propagating in free space with an animation region larger than the container demonstrate that the wave is not confined by the container (Fig. 4) whereas the wave that is propagating in a dielectric is much more confined to the container (Fig. 6). Widening electric boundaries and spacing them close together was able to approximate the plane wave behavior (Fig. 7)

In free space the simulation allowed us to calculate the phase velocity of the wave from the change in distance over the change in time. As expected the wave propagated at the speed of light. In the dielectric, we were able to calculate α from the \ln of the ratio of the electric field amplitudes at two points divided by the distance between the points, and β from 2π divided by the wavelength.

Both numbers matched the theoretical calculations. Since the experimentally calculated α and β matched the theoretical α and β , the Helmholtz wave equation is experimentally verified.

References

- [1] P. P. M. So, *Laboratory Manual for ELEC340 - Applied Electromagnetics and Photonics*, University of Victoria, 2016.